REFERENCES

Agency for Toxic Substances and Disease Registry. 2001. Chromium [online]. Available from: http://www.atsdr.cdc.gov/tfacts7.html.

American Society for Testing and Materials. 1998. ASTM protective coating inspection standards for field and shop applications, 2nd ed.

Amornchat, P. 2004. Preparation of titanium dioxide thin film on stainless steel plate using sol-gel technique for photocatalytic reduction of Cr (VI). Mater's Thesis, Graduate School, Chulalongkorn University. Bangkok. Thailand

Anh, Y. U., Kim, E. J., Kim, H. T. and Hahn, S. H. 2003. Variaiton of structural and optical properties of sol-gel TiO_2 thin films with catalyst concentration and calcination temperature. Materials Letters 57: 4660-4666.

Andreozzi, R., Caprio, V3., Insola, A. and Marotta, R. 1999. Advanced oxidation processes (AOP) for water purification and recovery. Catalysis Today 53: 51-59.

Ao, C. H., Lee, S. C. and Yu, J. C. 2003. Photocatalyst TiO_2 supported on glass fiber for indoor air purification: effect of NO on the photodegradation of CO and NO_2. Journal of Photochemistry and Photobiology Analysis: Chem 156: 171-177.

Bahnemann, D., Dillert, R., Dzengel, J., Goslich, R., Sagawe, G. and Schumacher, H.-W. 1999. Field studies of solar water detoxification using non light concentrating reactors. Journal of Advanced Oxidation Technology 4.

Blake, D. M., Webb, J., Turchi, C. and Magrini, K. 1991. Kinetic and mechanistic overview of TRiO2- photocatalyzed oxidation reactions in aqueous solution. Solar Energy Materials 24: 584-593.

Brinker, C. J., and Scherer, G. W. 1990. Sol-gel science: the physics and chemistry of sol-gel processing. San Diego. California. USA: Academic Press.

Chan, A. H. C., Chan, C. K., Barford, J. P. and Porter, J. F. 2002. Solar photocatalytic thin film cascade reactor for treatment of benzoic acid containing wastewater. Water Research 37: 1125-1135.

Chan, Y., Chen, J. and Lu, M. 2000. Intermediate inhibition in the heterogeneous UV-catalysis using a TiO_2 suspension system. Chemosphere 45: 29-35.

Chang, H. T., Wu, N. and Zhu, F. 2000. A kinetic model for photocatalytic degradation of organic contaminants in a thin-film TiO_2 catalyst. Pergamon 34, 2: 407-416.

Chenthamarakshan, C. R., and Rajeshwar, K. 1999. Heterogeneous photocatalytic reduction of Cr (VI) in UV-Irradiated titania suspensions: effect of protons, ammonium ions, and other interfacial aspects. Langmuir 2000 16: 2715-2721.

Clesceri, L. S., Greenberg, A. E. and Eaton, A. D. 1998. Standard methods for the examination of water and wastewater 20th edition 1998. Washington. America: American Public Health Association: 3-65-3-67.

Dijkstra, M. F. J., Michorius, A., Buwalda, H., Panneman, H. J., Winkelman, J. G. M. and Beenackers, A. A. C. M. 2001a. Comparison of the efficiency of immobilized and suspended systems in photocatalytic degradation. Catalysis Today 66: 487-494.

Dijkstra, M. F. J., Buwalda, H., De Jong, A. W. F., Michorius, A., Winkelman, J. G. M. and Beenackers, A. A. C. M. 2001b. Experimental comparison of three reactor designs for photocatalytic water purification. Chemical Engineering Science 56: 547-555.

Dijkstra, M. F. J., Panneman, H. J., Winkelman, J. G. M., Kelly, J. J. and Beenackers, A. A. C. M. 2002. Modeling the photocatalytic degradation of formic acid in a reactor with immobilized catalyst. Chemical Engineering Science 57: 4895-4907.

Dionysiou, D. D., Balasubramanian, G., Suidan, M. T., Khodadoust, A. P., Baudin, I., and Laine, J.-M. 1999. Rotating disk photocatalytic reactor: development, characterization and evaluation for the destruction of organic pollutants in water. Water Research 34, 11: 2927-2940.

Djaoued, Y., Badilescu, S., Ashrit, P. V., Bersani, D., Lottici, P. P. and Robichaud, J. 2002. Study of anatase to rutile phase transition in nanocrystalline titania films. Journal of Sol-Gel Science and Technology 24: 255-264.

Feitz, A. J., Boyden, B. H. and Waite, T. D. 2000. Evaluation of two solar pilot scale fixed bed photocatalytic reactors. Water Research 34, 16: 3927-3932.

Freudenhammer, H., Bahemann, D., Bousselmi, L., Geissen, S.-U., Ghrabi, A., Saleh, F., Si-Salah, A., Siemon, U. and Vogelpohl, A. 1998. Detoxification and recycling of wastewater by solar-catalytic treatment. Water Science and Technology 35, 4: 149-156.

Fu, H., Lu, G. and Li, S. 1998. Adsorption and photo-induced reduction of Cr (VI) ion in Cr(VI)-4CP (4-chlorophenol) aqueous system in the presence of TiO_2 as photocatalyst. Journal of Photochemistry and Photobiology 114: 81-88.

Fujishima, A., Hashimoto, K., and Watanabe, T. 1999. TiO_2 photocatalysis: Fundamental and application. Tokyo. Japan: BKC.

Gimenez, J., Aguado, M. A. and March, S. 1995. Photocatalytic reduction of chromium (VI) with titania powders in a flow system: Kinetics and catalyst activity. Journal of Molecular Catalysis 105: 67-78.

Guillard, C., Beaugiraud, B., Dutriez, C., Herrmann, J.-M., Jaffrezic, H., Jaffrezic-Renault, N. and Lacroix, M. 2002. Physicochemical properties and photocatalytic activities of TiO_2-films prepared by sol-gel methods. Applied Catalysis 39: 331-342.

Ha, H.Y. and Anderson, M.A. 1996. Photocatalytic degradation of formic acid via metal-supported titania. Journal of Environmental Engineering 122: 217-221.

Herrmann, J., M. 1999. Heterogeneous photocatalysis: fundamentals and applications to the removal of various types of aqueous pollutants. Catalysis Today 53: 115-129.

Hoffmann, M. R., Martin S. T., Choi W. And Bahneman, D. W. 1995. Environmental applications of semiconductor photocatalysis. Chemical Research 95: 69-96.

Horikoshi, S., Satou, Y., Hidaka, H. and Serpone, N. 2001. Enhanced photocurrent generation and photooxidation of benzene sulfonate in a continuous flow reactor using hybrid TiO_2 thin films immobilized on OTE electrodes. Journal of Photochemistry and Photobiology A: Chemistry 146: 109-119.

Hu, L., Yoko, T., Kozuka, H. and Sukka, S. 1992. Effects of solvent on properties of sol-gel derived TiO_2 coating films. Thin Solid Films 219: 18-23.

Kajitvitchyanukul, P., Ananpattarachai, J. and Pongpom, S. 2005. Sol-gel preparation and properties study of TiO_2 thin film for photocatalytic reduction of chromium (VI) in photocatalysis process. Science and Technology of Advanced Materials: 1-7.

Kajitvitchyanukul, P. and Watcharenwong, A. 2005. Role of pH, organic and inorganic ions on photocatalytic reduction of chromium (VI) using TiO_2 and ultraviolet light. ASEAN Journal on Science &Technology for Development (AJSTD) 22: 169-179

Khalil, L. B., Mourad, W. E. and Rophael, M. W. 1998. Photocatalytic reduction of environmental poluutant Cr (VI) over some semiconductors under UV/Visible light illumination. Applied catalysis 17: 267-273.

Kim, D. H., and Anderson, M. A. 1994. Photoelectrocatalytic degradation of formic acid using a porous TiO_2 thin film electrode. Environmental Science and Technology 28: 479-483.

Kim, D. J., Hahn, S. H., Oh, S. H. and Kim, E. J. 2001. Influence of calcination temperature on structural and optical properties of TiO_2 thin film prepared by sol-gel dip coating. Materials Letters 57: 355-360.

Ku, Y., and Jung, I. 2001. Photocatalytic reduction of Cr (VI) in aqueous solutions by UV irradiation with the presence of titanium dioxide. Water Research 35: 135-142.

Legrini, O., Oliveros, E. and Braun, A. M. 1993. Photochemical processes for water treatment. Chemical Reviews 93: 671-698.

Linsebigler, A. L., Lu, G. and Yates, J. T. 1995. Photocatalysis on TiO_2 surface: principles, mechanisms, and selected results. Chemical Reviews 95: 735-758.

Liqiang, J., Xiaojun, S., Weimin, C., Zili, X., Yaoguo, D. and Honggang, F. 2003. The preparation and characterization of nanoparticle TiO_2/Ti films and their photocatalytic activity. Journal of Physics and Chemistry of Solids 64: 615-623.

Litter, M. I. 1999. Review heterogenous photocatalysis transition metal ions in photocatalytic systems. Applied Catalysis B: Environmental 23: 89-114.

Lottiaux, M., Boulesteix, C., Nihoul, G., Varnier, F., Flory, F., Galindo, R. and Pelletier, E. 1989. Morphology and structure of TiO_2 thin layers VS thickness and substrate temperature. Thin Solid Films 170: 107-126.

Mehrvar, M., Anderson, W. A. and Moo-Young, M. 2002. Preliminary analysis of a tellerette packed-bed photocatalytic reactor. Advances in Environmental Research 6: 411-418.

Munter, R., Kallas, J., Preis, S., Trapido, M. and Veressinina, Y. 2001. Advanced oxidation processes (AOPs): a water treatment technology of the twenty-first century. Kemia-Kemi 5: 354-362.

National Safety Council. 1998. Chromium and chromium compounds chemical background [online]. Available from: http://www.osha.gov/SLTC/hexavalentchromium/recognition.html.

Negishi, N., Iyoda, T., Hashimot, K. and Fujishima, A. 1995. Preparation of transparent TiO_2 thin film photocatalyst and its photocatalytic activity. Chemical Letters 9: 841-842.

Nogueira, R. F. P. and Jardim, W. F. 1996. TiO_2 fixed bed reactor for water decontamination using solar light. Solar Energy 56, 5: 471-477.

Okamoto, K., Yamamoto, Y., Tanaka, H. and Itaya, A. 1985. Kinetics of hetero geneous photocatalytic decomposition of phenol over anatase TiO_2 powder. Bulletin of the Chemical Society of Japan 58: 2023-2028.

Ollis, D. F. 1991. Solar-assisted photocatalysis for water purification: issues, data, question. In Photochemistry Conversion and Storage of Solar Energy. Pelizzetti E. and Schiavello M. (Eds.): 593-622. Kluwer Academic Press, Netherlands.

Ollis, D. F. 2000. Photocatalytic purification and remediation of contaminated air and water. Chemistry 3: 405-411.

Ollis, D. F. and Turchi, C. S. 1990. Mixed reactant photocatalysis intermediates and mutual rate inhibition. Journal of Catalysis 119: 483-496.

Oppenländer, T. 2003. Photochemical Purification of Water and Air. Weinheim: WILEY-VCH.

Parsons, S. 2004. Advance oxidation processes for water and wastewater treatment. London. UK: IWA Publishing.

Pongpom, S. 2004. Preparation of titanium dioxide thin film on glass plate using sol-gel technique for photocatalytic reduction of Cr (VI). Mater's Thesis, Graduate School, Chulalongkorn University. Bangkok. Thailand.

Pozzo, R. L., Baltanas, M. A. and Cassano, A. E. 1997. Supported titanium dioxide as photocatalyst in water decontamination: State of the art. Catalysis Today 39: 219-231.

Rodenas, L. A. F., Weisz, A. D., Magaz, G. E. and Miguel, A. B. 2000. Effect of light on the electrokinetic behavior of TiO_2 particles in contact with Cr (VI) aqueous solutions. Journal of Colloid and Interface Science 230: 181-185.

Roquerol, F., Ronquerol, J. and Sing, K. 1998. Adsorption by Powders and Porous Solids. New York: Academic Press.

Sanpakal, B. R., Lux-Steiner, M. Ch. and Ennaoui, A. 2005. Synthesis and characterization of anatase- TiO_2 thin films. Applied Surface Science 239: 165-170.

Schrank, S. G., Jose, H. J. and Moreira, R. F. P. M. 2001. Simultaneous photocatalytic Cr (VI) reduction and dye oxidation in a TiO_2 slurry reactor. Journal of Photochemistry and Photobiology A: Chemistry 147: 71-76.

Shang, J., Li, W. and Zhu, Y. 2003. Structure and photocatalytic characteristics of TiO_2 film photocatalyst coated on stainless steel webnet. Journal of Molecule Catalysis 202: 187-195.

Shephard, G. S., Stockenstrom, S., Villiers, D., Engelbrecht, W. J. and Wessels. 2002. Degradation of microcystin toxins in a falling film photocatalytic reactor with immobilized titanium dioxide catalyst. Water Research 36: 140-146.

Sonawane, R. S., Hegde, S. G. and Dongare, M. K. 2002. Preparation of titanium (IV) oxide thin film photocatalyst by sol-gel dip coating. Materials Chemistry and Physics 77: 744-750.

Turprakay, S. and Liengcharernsit, W. 2005. Life time and regenation of immobilized titania for photocatalytic removal of aqueous hexavalent chromium. Journal of Hazardous Materials 124: 53-58.

U.S. Environmental Protection Agency. 1987. Federal Registration 52: 12866.

Venkata Subba Rao, K., Rachel, A., Subrahmanyam, M. and Boule, P. 2003. Immobilization of TiO_2 on pumice stone for the photocatalytic degradation of dyes and dye industry pollutants. Applied Catalysis 46: 77-85.

Watcharenwong, A. 2003. Removal of Chromium (VI) from synthetic wastewater using powdered TiO_2 in photocatalysis process. Master's Thesis, Department of Environmental Engineering, King Mongkut's University of Technology Thonburi, Bangkok, Thailand.

Weng, C. H., Wang, J. H. and Huang, C. P. 1997. Adsorption of Cr(VI) onto TiO_2 from dilute aqueous solutions. Water Science Technology 35: 55-62.

Xu, X. R., Li, H. B. and Gu, J. 2005. Simultaneous decontamination of hexavalent chromium and methyl *tert*-butyl ether by UV/TiO_2 process. Chemosphere.

Yoko, T., Yuasa, A., Kamiya, K., and Sakka, S. 1991. Sol-gel derived titanium dioxide film semiconductor electrode for photocleavage of water: Preparation and effects of post heating treatment on the photoelectrochemical behavior. Journal of Electrochemical Society 138: 2279-2284.

Yoko, T., Hu, L., Kozuka, H. and Sakka, S. 1995. Photoelectrochemical properties of TiO_2 coating films prepared using different solvents by the sol-gel method. Thin Solid Films 283: 188-195.

Yu, G., Zhu, W., Yang, Z., and Li, Z. 1998. Semiconductor photocatalytic oxidation of H-acid aqueous solution. Chemosphere 36:2673-2681.

Yu, J. and Zhao, X. 2000. Effect of substrates on the photocatalytic activity of nanometer TiO_2 thin films. Materials Research Bulletin 35: 1293-1301.

Yu, J., Zhao, X. and Zhao, Q. 2001. Photocatalytic activity of nanometer TiO_2 thin films prepared by the sol-gel method. Materials Chemistry and Physics 69: 25-29.

Zhang, L., Zhu, Y., He, Y. and Sun, H. 2003. Preparation and performances of mesoporous TiO_2 film photocatalyst supported on stainless steel. Applied Catalysis B: Environ 40: 287-292.

Zheng, S., Xu, Z., Wang, Y., Wei, Z. and Wang, B. A. 2000. On the enhance catalytic activity of TiO_2 supported layered compounds for Cr (VI) photo-reduction. Journal of photochemistry and photobiology 137:185-189.

Zhu, Y., Zhang, L., Wang, L., Fu, Y. and Cao, L. 2001. The prepartion and chemical structure of TiO_2 film photocatalysts supported on stainless steel substrates via the sol-gel method. Journal of Materials Chemistry 11: 1864-1868.

http://dev.nsta.org/evwebs/ 1952/photocatalysis.htm: Available: Oct 25, 2005

http://www.ecodevice.co.jp/borders/Bandgap-E.gif: Available: Oct 25, 2005

http://www.chemat.com/assets/ images/Flowchat72.jpg: Available: Feb 20, 2006

APPENDICES

APPENDIX A

STANDARD TEST METHOD

1. Colorimetric method

1.1 Principle

This method was used to measure only hexavalent chromium (Cr^{6+}). The hexavalent chromium is determined via the reaction with diphenylcarbazide in acidic condition. Complex of unknown composition produces a red-violet color. The reaction is very sensitive which is measured at 540 nm.

1.2 Apparatus

The following are required:

1.2.1 ***Spectrophotometer***, for use at 540 nm, with a light path of 1 cm or longer.

1.2.2 ***Acid-washed glassware***: new and unscratched glassware will adsorb chromium on glass surfaces during the procedure. Thoroughly, other used glassware and new glassware will be cleaned with nitric or hydrochloric acid to remove chromium traces.

1.3 Reagents

1.3.1 ***Stock chromium solution***: Dissolve 141.4 mg $K_2Cr_2O_7$ in distilled water and dilute to 100 ml; 1 ml = 500 μg Cr.

1.3.2 ***Standard chromium solution***: Dilute 10 ml stock chromium solution to 100 ml; 1 ml = 50 μg Cr.

1.3.3 ***Nitric acid***, HNO_3, conc.

1.3.4 ***Sulfuric acid***, H_2SO_4, 0.2 N: Dilute 17 ml 6 N H_2SO_4 to 500 ml with distilled water.

1.3.5 ***Phosphoric acid***, H_3PO_4, conc.

1.3.6 ***Diphenylcarbazide solution***: Dissolve 250 mg 1,5-diphenylcarbazide (1,5-diphenylcarbohydrazide) in 50 ml acetone. Store in a brown bottle. Discard when solution becomes discolored.

1.4 Procedures

1.4.1 Preparation of calibration curve

- Pipet measured volumes of standard chromium solution (50 μg/ml) ranging from 1 to 100 ml, to provide standards for 0.5 to 50 μg Cr, into 100-ml volumetric flasks,
- Add H_3PO_4 0.25 ml,
- Adjust pH to 1 by 0.2 N H_2SO_4,
- Dilute with distilled water into volumetric flasks 100 ml,
- Add diphenylcarbazide 2 ml into volumetric flasks,
- Wait 5 minutes to get a complete color,
- Trasfer an appropriate portion to a 1 cm absorption cell and measure the absorbance at 540 nm, using the distilled water as a reference,
- Measure the absorbance by a UV-Visible spectrophotometer,
- Correct absorbance reading by subtracting absorbance of a blank carrier through the method,
- Make a calibration curve by plotting corrected absorbance against micrograms of chromium.

1.4.2 Sample measurement

- Take the sample 5 ml,
- Add H_3PO_4 0.25 ml,
- Adjust pH to 1 by 0.2 N H_2SO_4,
- Dilute with distilled water into volumetric flasks 100 ml,
- Add diphenylcarbazide 2 ml into volumetric flasks,
- Wait 5 minutes to get a complete color,
- Trasfer an appropriate portion to a 1 cm absorption cell and measure the absorbance at 540 nm, using the distilled water as a reference,
- Measure the absorbance by a UV-Visible spectrophotometer,
- Correct absorbance reading by subtracting absorbance of a blank carrier through the method.

APPENDIX B

CALCULATION OF CRYSTALLITE SIZE

Calculation of crystallite size by Debye-Scherrer equation

The size of anatase crystallite in this study was calculated from the half maximum height width of the 101 diffraction peak of anatase using the Debye-Scherrer equation. The value of the shape factor, K was taken to be 0.89.

The Debye-Scherrer equation was shown as below:

$$L = K\lambda / \beta \cos \theta$$

Where;

L	=	the crystalline size (nm)
K	=	the Debye-Scherrer constant (usually taken as 0.89)
λ	=	the wavelength of the x-ray radiation (Cu Kα = 0.15418)
β	=	the line width at half-maximum height of the broadened peak
θ	=	the half diffraction angle of the centroid of the peak (degree)

For instance, the calculation of the crystallite size of anatase TiO_2 phase was dedicated as follows:

From;

β	=	0.00733 radian
θ	=	12.65°
λ	=	0.15418 nm

So;

$$L = (0.89 \times 0.15418) / (0.00733 \times \text{Cos } 12.65)$$

$$= 19.19 \text{ nm}$$

APPENDIX C

SPECIAL EQUIPMENT

1. Scanning Electron Microscope (SEM)

The Scanning Electron Microscope, or SEM, is an incredible tool for seeing the unseen worlds of microspace. Electron microscopy takes advantage of the wave nature of rapidly moving electrons. Where visible light has wavelengths from 4,000 to 7,000 Angstroms, electrons accelerated to 10,000 KeV have a wavelength of 0.12 Angstroms. Optical microscopes have their resolution limited by the diffraction of light to about 1000 diameters magnification. Electron microscopes, so far, are limited to magnifications of around 1,000,000 diameters, primarily because of spherical and chromatic aberrations. Scanning electron microscope resolutions are currently limited to around 25 Angstroms, though, for a variety of reasons.

1.1 The principle of SEM

A scanning electron microscope creates high resolution, three dimensional images of a sample's surface. The sample, often gold-coated for electroconductivity, is bombarded with a focused beam of electrons which liberates secondary electrons from the sample's surface. A detector in the microscope systematically "counts" these electrons, recording data on their origin and emission intensity which can then be assembled into a high contrast, high resolution image.

The scanning electron microscope generates a beam of electrons in a vacuum. That beam is collimated by electromagnetic condenser lenses, focused by an objective lens, and scanned across the surface of the sample by electromagnetic deflection coils. The primary imaging method is by collecting secondary electrons that are released by the sample. The secondary electrons are detected by a scintillation material that produces

flashes of light from the electrons. The light flashes are then detected and amplified by a photomultiplier tube.

By correlating the sample scan position with the resulting signal, an image can be formed that is strikingly similar to what would be seen through an optical microscope. The illumination and shadow show a quite natural looking surface topography.

There are other imaging modes available in the SEM. Specimen current imaging using the intensity of the electrical current induced in the specimen by the illuminating electron beam to produce an image. It can often be used to show subsurface defects. Backscatter imaging uses high energy electrons that emerge nearly 180 degrees from the illuminating beam direction. The backscatter electron yield is a function of the average atomic number of each point on the sample, and thus can give compositional information.

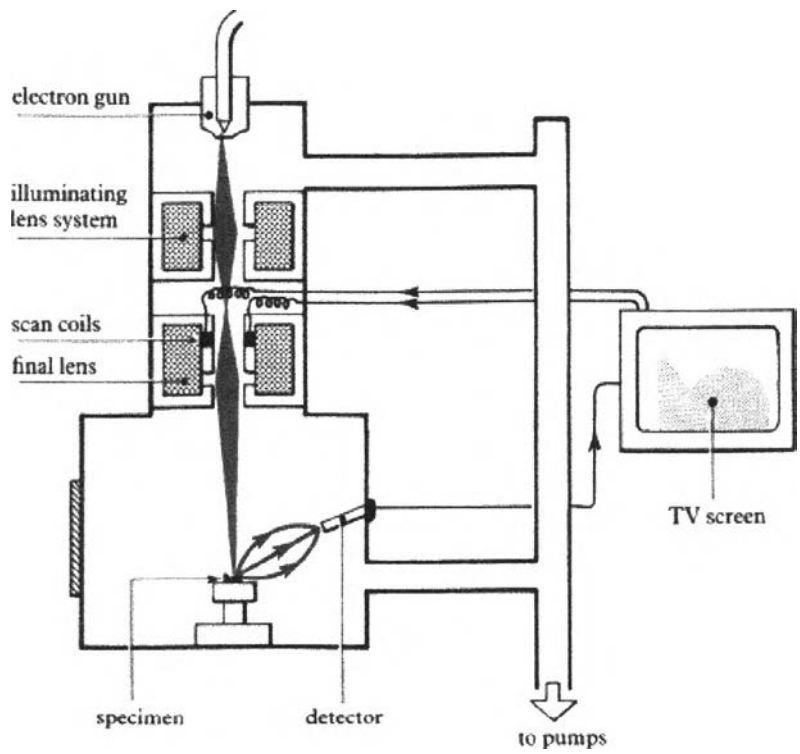

Figure C-1 Schematic drawing of a scanning electron microscope with secondary electrons forming the images on the TV screen.
(http://acept.la.asu.edu/PiN/rdg/elmicr/elmicr.shtml: Available on Mar 4, 2006)

1.2 Sample preparation

Samples have to be prepared carefully to withstand the vacuum inside the microscope. Surface topology, such as in fractography, may require no sample preparation if the specimen can withstand the low chamber pressure and electron beam bombardment of the SEM. The microstructure may be greatly enhanced, however, by such methods as polishing and selective etching of the surface. Most SEMs have sample chambers with limited dimensions, and the specimen must be affixed to a stage holder for orientation and manipulation within the chamber. Conductive adhesives with low vapor pressure or mechanical devices are used to mount the specimen. Special chambers and stages are available to suit most needs.

The most common form of sample preparation for the SEM is the deposition of a metal thin film onto the specimen surface. Vacuum evaporation and ion sputtering of metals are common methods of depositing these thin films (Goldstein et al., 1992). The metal thin film provides electrical conductivity, enhances the signal (if a higher-*Z* metal is used), and may add strength to the specimen.

2. Field Emission Scanning Electron Microscopy (FE-SEM)

Resolution of 1 nm is now achievable from an SEM with a field emission (FE) electron gun. Magnification is a function of the scanning system rather than the lenses, and therefore a surface in focus can be imaged at a wide range of magnifications from 3× up to 150,000×.

FE-SEM is the abbreviation of the word Field Emission Scanning Electron Microscope. Scanning and electron transmission microscopes (SEM and TEM) use as a source for image formation electrons (particles with a negative charge), in contrast to light microscopes (LM). These electrons are produced by a Field emission source in a FE-SEM. The sample (object) is scanned in a kind of zig-zag pattern by an electron beam.

Modern SEMs with field emission electron guns (FE-SEMs) are capable of resolutions near 1 nm on appropriate samples using the SE signal. Tungsten filament instruments can routinely obtain resolutions of 3 to 4 nm on appropriate specimens. Samples that require special conditions, such as low voltage or low dosage, and samples that are inherently poor signal generators due to their composition may fall far short of this resolution. The signal from these specimens can often be enhanced by depositing a thin film of metal such as chromium or gold onto the surface. This increases contrast in the SE signal and allows for higher resolution imaging. Operating conditions that favor one signal, for instance, the high beam currents and energies used for x-ray analysis, can also reduce image resolution. High-resolution BSE images can be obtained by selecting only high-energy BSEs (low-energy-loss BSEs), since these have undergone few interactions with the sample and are thus from a smaller sampling volume.

The FE-SEM deserves special mention due to its enormous impact on the field. The field emission (FE) electron gun allows for the creation of an exceptionally bright (small with high-current-density) electron beam. This in itself has made scanning electron microscopy competitive with transmission electron microscopy for materials characterization in the nanometer range. The FE source is often coupled with a special lens design such that the specimen is in the field of the lens and the detector is within the column rather than the sample chamber. The FESEM also has the ability to produce a small probe diameter at low voltage, opening the way to many applications that were difficult with thermionic electron guns (Greenhut and Friel, 1997). Low-voltage scanning electron microscopy has the advantage of revealing more details of the surface since there is less penetration of the beam into the specimen and is less damaging to the material. The SE yield from the specimen is a function of voltage, and at lower beam voltages the specimen reaches a point at which emission of secondary and backscattered electrons equals the beam current. This is a unique voltage for each material at which there is no specimen charging, and the surface can be imaged without a conductive coating. This phenomenon has also been used as a voltage contrast mechanism in materials such as copolymers and ceramic composites that were traditionally difficult to observe with the SEM.

3. X-Ray Diffraction (XRD)

X-ray Diffraction (XRD) is a powerful non-destructive technique for characterizing crystalline materials. It provides information on structures, phases, preferred crystal orientations (texture) and other structural parameters such as average grain size, crystallinity, strain and crystal defects. X-ray diffraction peaks are produced by constructive interference of monochromatic beam scattered from each set of lattice planes at specific angles. The peak intensities are determined by the atomic decoration within the lattice planes. Consequently, the X-ray diffraction pattern is the fingerprint of periodic atomic arrangements in a given material. An on-line search of a standard database for X-ray powder diffraction pattern enables quick phase identification for a large variety of crystalline samples.

3.1 Main Applications

- Determination of phase contents of reaction products.
- Measurement of average crystallite size, strain or micro-strain effects in bulk and thin-film samples.
- Quantification of preferred orientation (texture) in thin films and multi-layers.
- Refinement of lattice parameters.
- Measurement of residue stress in blank film stacks and patterned wafers.
- Determination of thickness, interface roughness and density for thin films and multi-layers.

3.2 The principle of X-ray diffraction

3.2.1 Diffraction and Bragg equation

X-ray diffraction analysis uses the property of crystal lattices to diffract monochromatic X-ray light. This involves the occurrence of interferences of the waves scattered at the successive planes, which are described by Bragg's equation:

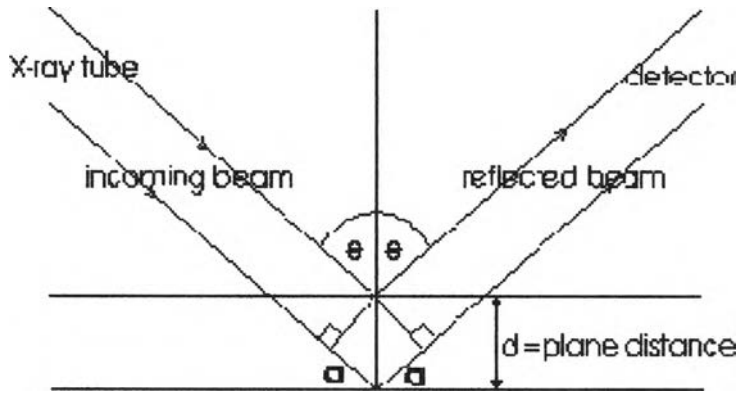

Figure C-2 The principle of X-ray diffraction

(http://www.mastest.com/xrdxrr.htm: Available on Mar 4, 2006)

W.L. Bragg (early 1900's) studied that the diffracted x-rays act as if they were "reflected" from a family of planes within crystals. Bragg's planes are the rows of atoms that make the crystal structure. These "reflections" were indicated to only occur under certain conditions, which satisfy the equation:

$$n\lambda = 2d \sin \Theta \qquad \textbf{(Bragg's equation)}$$

Where;

n = an integer (1, 2, 3, ..., n)

λ = the wavelength in Angstroms (1.54 A° for Cu)

d = the distance between atomic planes

θ = the angle of incidence of the x-ray beam and the atomic planes.

3.2.2 X-ray spectra

X-rays are a small part of the electromagnetic spectrum with ranging wavelengths from 0.02 A° to 100 A° (A° = Angstroms = 10^{-8} m). The crystal is studied to find the λ on the order from 1 to 2 A°, i.e. Copper Ka = 1.5418 A°. In the visible region, it is given the

larger λ (4000 – 7200 A°); however, x-ray make such energy, it can penetrate deeper into a material. The Einstein's equation can be explained this circumstance easily, $E = h\upsilon = hc/\lambda$; E is the energy, υ is the frequency, c is the speed of light which is constant for an electromagnetic radiation, λ is the wavelength and h is the Plank's constant.

3.2.3 XRD technique in thin film analysis

Thin films deposited by various methods show varying degrees of anisotropy. This information relating preferred crystallite orientation (or texture) can be quantified and evaluated by XRD methods. With certain thin film devices, the direction and degree of preferred orientation of the film in relation to the substrate can influence the functionality of the device.

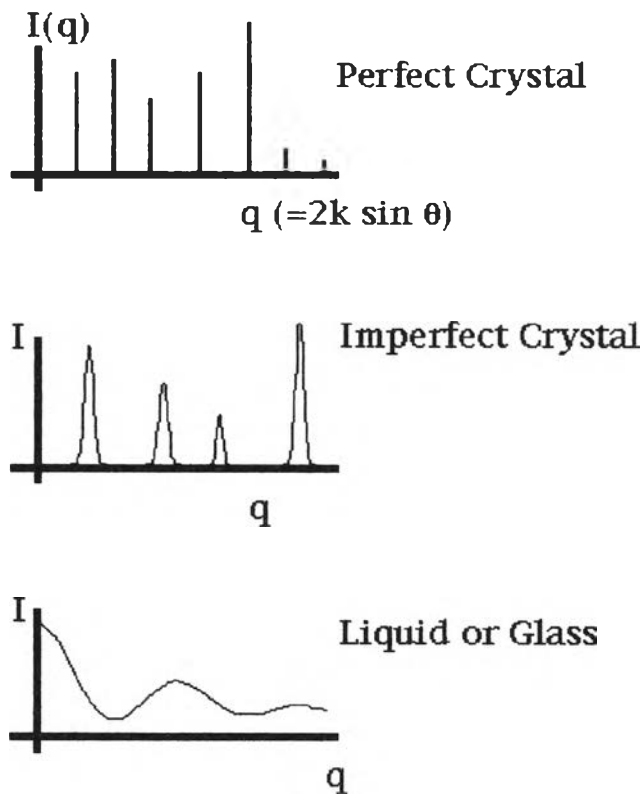

Figure C-3 The example of XRD spectra

4. Ultraviolet and Visible Spectroscopy

Many molecules absorb ultraviolet or visible light. The absorbance of a solution increases as attenuation of the beam increases. Absorbance is directly proportional to the path length, b, and the concentration, c, of the absorbing species.

Beer's Law states that $A = \varepsilon bc$, where ε is a constant of proportionality, called the absorbtivity. Different molecules absorb radiation of different wavelengths. An absorption spectrum will show a number of absorption bands corresponding to structural groups within the molecule. For example, the absorption that is observed in the UV region for the carbonyl group in acetone is of the same wavelength as the absorption from the carbonyl group in diethyl ketone.

4.1 The principle of UV-Visible spectroscopy

When either light, visible or ultraviolet, is absorbed by valence (outer) electrons these electrons are promoted from their normal (ground) states to higher energy (excited) states (Figure C-4). The energies of the orbitals involved in electronic transitions have fixed values. Because energy is quantised, it seems safe to assume that absorption peaks in a UV/visible spectrum will be sharp peaks. However, this is rarely, if ever, observed. Instead the spectrum has broad peaks. This is because there are also vibrational and rotational energy levels available to absorbing materials (Figure C-4).

Because light absorption can occur over a wide range, light from 190 nm to 900 nm is usually used. Valence electrons are found in three types of electron orbitals. Single, or σ, bonding orbitals; double or triple (π bonding orbitals); and non-bonding orbitals (lone pair electrons). Sigma (σ) bonding orbitals tend to be lower in energy than π bonding orbitals, which in turn are lower in energy than non-bonding orbitals. When electromagnetic radiation of the correct frequency is absorbed a transition occurs from one of these orbitals to an empty orbital, usually an antibonding orbital – σ^* or π^* – (Figure C-5). Most of the transitions from bonding orbitals are too high a frequency (too

short a wavelength to measure easily), so most of the absorptions involve only $\pi \rightarrow \pi^*$, $n \rightarrow \sigma^*$ and $n \rightarrow \pi^*$ transitions.

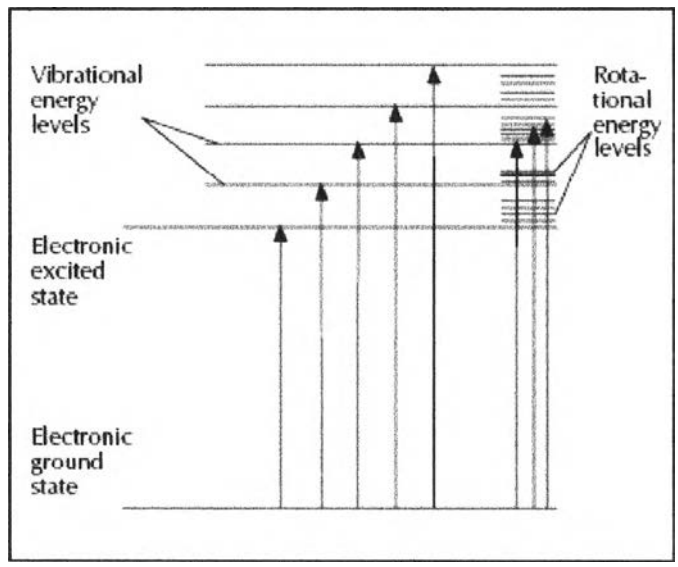

Figure C-4 The scheme of the energy promoted the electrons with different motion

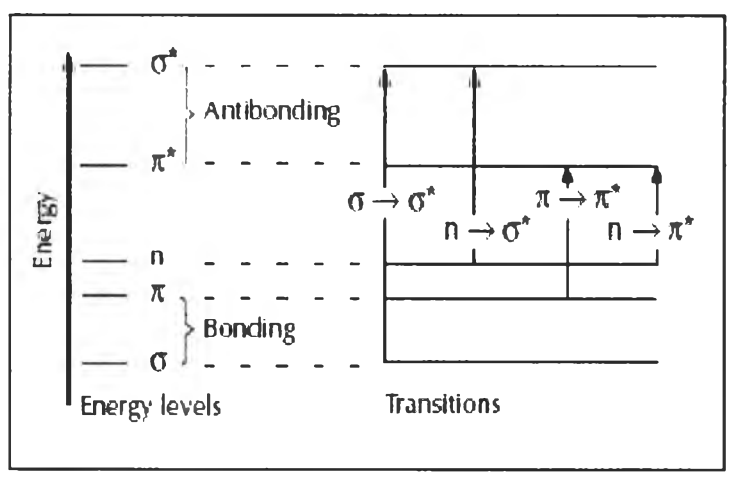

Figure C-5 The diagram of the energy levels

4.2 Measuring techniques

There are two types of analysis which are qualitative analysis and quantitative analysis using in this technique. All samples can be determined when the molecular absorption conducts. A couple of techniques would be demonstrated as follow:

4.2.1 Qualitative analysis

All analysts may be identified by comparing the absorption spectra of the unknown substance with the graphs of the known spectra. Moreover, it can be used to specify two or more analysts at the same time.

4.2.2 Quantitative analysis

A known analyst can be determined by measuring the absorbance at one or more than one wavelengths and taking the molar absorption coefficient to calculate its concentration. However, the concentration can definitely be found from an analytical calibration curve that is contained by plotting the measured absorbance of various reference solutions according to their exact concentrations. A graph of absorbance against concentration is a straight line passing through the origin if the Beer-Lambert law is applied.

APPENDIX D

EXPERIMENTAL DATA

Table D-1 The absorbance of residual Cr (VI) in the photocatalytic reduction using thin film TiO_2 prepared with and without Acetyl acetone.

Irradiation time (min)	Absorbance of residual Cr (VI) (mg/L)							
	TiO_2 without Acetyl acetone				TiO_2 with Acetyl acetone			
	1 st	2 nd	average	C/Co	1 st	2 nd	average	C/Co
0	25.00	25.00	25.00	1.00	25.00	25.00	25.00	1.00
15	22.20	21.92	21.01	0.88	19.51	20.54	20.03	0.80
25	20.77	21.24	18.62	0.84	18.06	19.51	18.79	0.75
35	17.48	19.76	17.29	0.74	13.90	17.86	15.88	0.63
45	16.44	18.15	16.26	0.69	12.58	15.59	14.08	0.56
60	15.45	17.06	14.01	0.65	9.49	11.60	10.55	0.42
75	13.23	14.80	10.35	0.56	6.28	7.77	7.03	0.28
105	9.17	11.54	6.62	0.41	1.78	3.26	2.52	0.10
135	5.21	8.02	3.04	0.26	0.00	0.00	0.00	0.00
165	1.23	4.84	0.00	0.12	0.00	0.00	0.00	0.00
195	0.00	1.41	0.00	0.00	0.00	0.00	0.00	0.00

Table D-2 The absorbance of residual Cr (VI) in the photocatalytic reduction using thin film TiO_2 calcined at various temperatures.

Irradiation time (min)	Absorbance of residual Cr (VI) (mg/L)															
	300 °C				400 °C				450 °C				500 °C			
	1 st	2 nd	av	C/Co	1 st	2 nd	av	C/Co	1 st	2 nd	av	C/Co	1 st	2 nd	av	C/Co
0	25.00	25.00	25.00	1.00	25.00	25.00	25.00	1.00	25.00	25.00	25.00	1.00	25.00	25.00	25.00	1.00
15	20.11	21.98	21.04	0.84	18.85	21.90	20.37	0.81	18.72	21.00	09.86	0.79	19.51	20.54	20.03	0.80
25	18.19	20.87	19.53	0.78	17.26	19.04	18.15	0.73	18.34	19.97	19.16	0.77	18.07	19.51	18.79	0.75
35	15.72	19.90	17.82	0.71	15.26	18.09	16.68	0.67	16.08	18.54	17.31	0.69	13.90	17.86	15.88	0.64
45	13.33	18.87	16.10	0.64	13.42	15.72	14.57	0.58	13.89	15.69	14.79	0.59	12.58	15.59	14.08	0.56
60	11.52	16.37	13.94	0.56	10.64	14.24	12.44	0.50	10.68	12.76	11.72	0.47	9.49	11.60	10.55	0.42
75	7.90	14.89	11.40	0.46	8.15	12.07	10.11	0.40	7.61	9.73	8.70	0.35	6.28	7.77	7.03	0.28
105	3.37	11.13	7.25	0.29	3.85	10.27	7.06	0.28	2.14	4.78	3.46	0.14	1.78	3.26	2.52	0.10
135	0.00	7.78			0.00	6.94			0.00	2.63			0.00	0.00		
165	0.00	4.09			0.00	3.25			0.00	0.00			0.00	0.00		
195	0.00	0.21			0.00	0.00			0.00	0.00			0.00	0.00		

Table D-3 The absorbance of residual Cr (VI) in the photocatalytic reduction using thin film TiO_2 derived with different coating cycles.

Irradiation time (min)	Absorbance of residual Cr (VI) (mg/L)											
	1 cycle				2 cycles				3 cycles			
	1 st	2 nd	av	C/Co	1 st	2 nd	av	C/Co	1 st	2 nd	av	C/Co
0	25.00	25.00	25.00	1.00	25.00	25.00	25.00	1.00	25.00	25.00	25.00	1.00
15	21.90	21.94	21.92	0.88	21.99	22.33	22.16	0.89	19.51	20.54	20.03	0.80
25	19.32	20.29	19.81	0.79	20.67	19.63	20.15	0.81	18.07	19.51	18.79	0.75
35	18.84	18.54	18.69	0.75	19.24	17.38	18.31	0.73	13.90	17.86	15.88	0.64
45	16.88	17.24	17.06	0.68	16.79	15.57	16.18	0.65	12.58	15.59	14.08	0.56
60	14.63	14.85	14.74	0.59	13.81	12.25	13.03	0.52	9.49	11.60	10.55	0.42
75	12.18	12.69	12.44	0.50	11.35	9.21	10.28	0.41	6.28	7.77	7.02	0.28
105	7.46	8.04	7.75	0.31	6.08	5.00	5.54	0.22	1.78	3.26	2.52	0.10
135	3.46	3.84	3.65	0.15	2.32	3.43	2.87	0.11	0.00	0.00		
165	0.25	0.33	0.29	0.01	0.00	0.00			0.00	0.00		
195	0.00	0.00	0.00		0.00	0.00			0.00	0.00		

Irradiation time (min)	Absorbance of residual Cr (VI) (mg/L)							
	4 cycles				5 cycles			
	1 st	2 nd	av	C/Co	1 st	2 nd	av	C/Co
0	25.00	25.00	25.00	1.00	25.00	25.00	25.00	1.00
15	20.12	21.66	20.89	0.84	21.21	20.94	21.08	0.84
25	17.80	19.57	18.68	0.75	19.51	18.99	19.25	0.77
35	15.78	17.66	16.72	0.67	17.66	17.49	17.58	0.70
45	13.76	15.47	14.62	0.58	16.42	16.64	16.53	0.66
60	11.27	12.71	11.99	0.48	14.27	15.49	14.88	0.60
75	9.09	10.58	9.83	0.39	11.98	13.48	12.73	0.51
105	5.49	6.00	5.74	0.23	8.01	9.84	8.93	0.36
135	2.35	1.90	2.13	0.09	4.28	6.23	5.25	0.21
165	0.00	0.00	0.00	0.00	1.75	2.00	1.87	0.07
195	0.00	0.00	0.00	0.00	0.00	0.00		

Table D-4 The absorbance of residual Cr (VI) in the photocatalytic reduction with different illumination wavelengths.

Irradiation time (min)	Absorbance of residual Cr (VI) (mg/L)											
	254 nm				380 nm				420 nm			
	1 st	2 nd	av	C/Co	1 st	2 nd	av	C/Co	1 st	2 nd	av	C/Co
0	25.00	25.00	25.00	1.00	25.00	25.00	25.00	1.00	25.00	25.00	25.00	1.00
15	21.70	22.09	21.90	0.88	19.51	20.54	20.03	0.80	23.42	22.15	22.78	0.91
25	18.88	19.05	18.97	0.76	18.07	19.51	18.79	0.75	21.94	21.63	21.78	0.87
35	17.30	16.66	16.98	0.68	13.90	17.86	15.88	0.64	20.77	19.65	20.21	0.81
45	14.62	14.30	14.46	0.58	12.58	15.59	14.08	0.56	19.80	19.41	19.60	0.78
60	12.26	11.06	11.66	0.47	9.49	11.60	10.55	0.42	17.27	18.67	17.97	0.72
75	8.36	8.76	8.56	0.34	6.28	7.77	7.02	0.28	17.11	16.80	16.96	0.68
105	4.09	4.32	4.21	0.17	1.78	3.26	2.52	0.10	15.06	14.45	14.76	0.59
135	0.00	0.00	0.00		0.00	0.00			12.20	11.92	12.06	0.48
165	0.00	0.00	0.00		0.00	0.00			9.79	9.45	9.62	0.38
195	0.00	0.00	0.00		0.00	0.00			6.83	5.99	6.41	0.26

BIOGRAPHY

Miss Apinya Tisavipaksakul was born on Aug 5, 1981 in Bangkok, Thailand. She got her Bachelor's degree in Chemistry from faculty of Science, Srinakharinwirot University in 2002. Then, she enrolled her Master's degree in the International Postgraduate Program in Environmental Management (Hazardous Waste Management), Inter-Department of Environmental Management, Chulalongkorn University, Bangkok, Thailand.